

Analysis of Echocardiography Images Using Applications of Image Processing Techniques: A Review

^{1*}Babita Dhiman, ²Surender Kumar Grewal

^{1,2}Department of ECE, DCRUST, Murthal (Sonapat), Haryana, India

Abstract: *Echocardiographic imaging is a medical imaging modality that uses ultrasound in order to obtain cross sectional views of the heart. In echocardiographic images, ultrasound images play a crucial role, because they are helpful to be produced at video-rate and therefore allow a dynamic analysis of moving structures. In this paper the ultrasound image segmentation methods are discussed by using echocardiographic images, in a broad sense, specially focusing on techniques developed for medical enhancement.*

Keywords: Echocardiographic images, Image processing Techniques, Segmentation method, Biomedical Applications, Clinical Applications

1. Introduction

Image analysis usually refers to processing of images by computer with the goal of finding what objects are presented in the image. Image segmentation is one of the most critical tasks in automatic image analysis. In a standard ultrasound system there are three basic types of data available for analysis:

- a) Radiofrequency (RF) signals,
- b) Envelope-detected signals,
- c) B-mode images.

A transmit/receive ultrasound transducer receives multiple analog radio-frequency (RF) signals which are converted to digital RF signals and beam formed into a single RF signal. The RF signal is then filtered, and envelope detection is performed to give an envelope-detected signal. Finally, the envelope-detected signal undergoes log compression, and often proprietary post-processing is applied to give a grayscale representation. The resulting signals are then interpolated and rasterized to give a B-mode or display image [1]. The basic problem in the use of echocardiography is the ability to obtain a reliable set of physical parameters related to cardiac status, so that assessment of heart disease can be performed automatically. In image processing using segmentation on echocardiographic images remains a necessary step to obtain qualitative measurements such as the location of objects of interest as well as for quantitative measurements as area, mass or the analysis of dynamic behavior of anatomical structures over time. These images are also beneficial because their acquisition is cheap and does not require ionizing radiations compared to other medical imaging techniques.

Further, the paper is organized as follows:

Firstly, the basic methods of image segmentation, forming of ultrasound images and also the histogram matching of the images will be discussed here. After that the discussion of the basics on ultrasound image segmentation will occur.

Moreover, Second section will explain here the ultrasonic image segmentation methods based on biomedical and clinical applications of image processing techniques.

2. Different Methods of Image Segmentation

Segmentation Algorithms mainly based on two basic properties:

1. Discontinuity (Edge based Approaches) : Based on abrupt change in Intensity
2. Similarity (Region based Approaches) : Similar according to predefined Criterion

A. Edge Based Approaches

Edge detection is a well-developed field on its own within image processing. Region boundaries and edges are closely related, since there is often a sharp adjustment in intensity at the region boundaries. Edge detection techniques have therefore been used as the base of another segmentation technique.

B. Similarity

Thresholding

Segmentation problems requiring multiple thresholds are best solved using region growing methods. Thresholding can be viewed as:

$$T = T[x, y, p(x, y), f(x, y)]$$

Where $f(x, y)$ is gray-level at (x, y) and $p(x, y)$ denotes some local property, for example average gray level in neighborhood.

A thresholded image $g(x, y)$ is defined as

$$g(x, y) =$$

$\begin{cases} 1 & \text{if } f(x, y) > T_y \\ 0 & \text{otherwise} \end{cases}$ where 1 is object and 0 is background

When $T = T[f(x, y)]$, threshold is global
 When $T = T[p(x, y), f(x, y)]$, threshold is local
 When $T = T[x, y, p(x, y), f(x, y)]$, threshold is dynamic.

Region-Based Segmentation Basic Formulation

Let R represent the entire image region. The segmentation process partitions R into n subregions, R_1, R_2, \dots, R_n , such that...

(a) $\bigcup_{i=1}^n R_i = R$ (b) R_i is a connected region, $i = 1, 2, \dots, n$ (c) $R_i \cap R_j = \emptyset$ for all i and j , $i \neq j$ (d) $\bigcap_{i=1}^n R_i \neq \emptyset$ (e) $\bigcup_{i=1}^n R_i = R$
 Here $P(R_i)$ is logical predicate defined over all points in R_j
 (a) Every pixel must be in a region (b) All the points in a region must be "connected" (c) Regions must be disjoint (d) For example $P(R_i) = \text{TRUE}$ if all the pixels in R_i have the same gray level (e) Regions R_i and R_j are different in some sense.

- Start from a set of seed points and from these points grow the regions by appending to each seed those neighboring pixels that have similar properties
- The selection of the seed points depends on the problem. When a priori information is not available, clustering techniques can be used: compute the above mentioned properties at every pixel and use the centroids of clusters
- The selection of similarity criteria depends on the problem under consideration and the type of image data that is available
- Descriptors must be used in conjunction with connectivity (adjacency) information
- Formulation of a "stopping rule". Growing a region should stop when no more pixels satisfy the criteria for inclusion in that region.
- When a model of the expected results is partially available, the consideration of additional criteria like the size of the region, the likeness between a candidate pixel and the pixels grown so far, and the shape of the region can improve the performance of the algorithm.

Region splitting and merging Subdivide an image initially into a set of arbitrary, disjoint regions and then merge and/or split the regions in an attempt to satisfy the necessary conditions. Let R represent entire image region and select a predicate P
 (1) Split into four disjoint quadrants any region R_i for which $\bigcap_{i=1}^4 R_i = \text{FALSE}$
 (2) Merge any adjacent regions R_j and R_k for which $\bigcup_{i=1}^4 R_i = \text{FALSE}$
 (3) Stop when no further merging or splitting is possible.

Split and merge Define $\bigcap_{i=1}^4 R_i = \text{TRUE}$ if at least 80% of the pixels in R_i have the property $|z_i - m_i| < 2\sigma_i$. If $\bigcap_{i=1}^4 R_i = \text{TRUE}$ the value of all the pixels in R_i are set equal to m_i . Splitting and merging are done using the algorithm on the previous transparency. Properties based on mean and standard deviation attempt to quantify the texture of a region. Texture segmentation is based on using measures of texture for the predicates $P(R_i)$. Segmentation algorithms have had fairly limited application in ultrasound imaging. High levels of speckling present in ultrasound images make accurate segmentations difficult. Furthermore, the real-time acquisition in ultrasound makes it better suited for motion estimation tasks ([3, 4]) where active contours,

because of their dynamic nature, are often used. Ultrasound is also often employed in detecting pathology using textural classifiers [5] but regions of interest are typically obtained through manual interaction. Nevertheless, some automated segmentation work has been performed in ultrasound for extracting a variety of structures. In [6], a thresholding of intensity and texture statistics was used to segment ovarian cysts. Deformable models have had good success in ultrasound applications such as in the segmentation of echocardiograms [7, 8, 9]. In [10], an active contour was used to determine the boundary of the calcaneus in broadband ultrasonic attenuation parameter images, which are less noisy than standard ultrasound images. In [12], deformable models were used to determine the boundary of the fetus and the fetus head respectively. Deformable models have also been used to segment cysts in ultrasound breast images. Other methods have been applied for the segmentation of coronary arteries in intravascular ultrasound images [13] and for segmenting the pubic arch in transrectal ultrasound [11].

3. Classification of Ultrasound Segmentation Based On Clinical Application

3.1 Echocardiography

Echocardiography is the application of ultrasound for imaging of the heart. Standard ultrasound techniques are used to image two-dimensional slices of the heart. Apart from 2-D, conventional echocardiography also employs M-mode and Doppler. Color Doppler is used to image flowing blood. Continuous wave Doppler and Pulsed wave Doppler are used to measure the velocity of flowing blood.

The quality of data, and hence challenges for segmentation, vary depending on the view due to the anisotropy of ultrasound image acquisition, artifacts such as shadowing from the lungs, and attenuation which can be strong. Segmentation methods should also have strategies for avoiding the papillary muscles. Reliably finding the outer wall (often called Epicardial border detection) is much more challenging, particularly from apical views. There are many papers on left ventricle tracking which deal with the tracking/deformation model independent of feature extraction or the imaging modality. Three-dimensional echocardiography facilitates spatial recognition of intracardiac structures, potentially enhancing diagnostic confidence of conventional echocardiography. Three-dimensional echocardiography requires the collection of a volumetric data set where each image (cut plane) is defined with respect to its exact position in space. Early work used either freehand ultrasound (with 2-D image acquisition synchronized with recording the location of the slice with a position sensor), rotational 3-D probes which acquired a sparse set of 2-D image sequences, or real-time 3-D echocardiography based on the Volumetric system.

Mishra et al. [2] proposed an active contour solution where the optimization was performed using a genetic algorithm. In a first image, the preprocessed contour after low pass

filtering and morphological operations is optimized using GA for rough boundary delineation at fixed number of sample points were used to define an initial estimate of the contour. A nonlinear mapping of the intensity gradient was used in the energy functional which is minimized. The final contour was used to initialize contour finding in the next time frame. Mignotte and Meunier choose to use a statistical external energy in a discrete active contour for the segmentation of short axis parasternal images, arguing that this was well-suited in ultrasound images with significant noise and missing boundaries. To this end, a shifted Rayleigh distribution was used to model gray levels statistics.

Level sets are often considered as an alternative to active contours and this approach has also been considered for echocardiographic image segmentation. Yan considered applying the level set method to echocardiographic images using an adaptation of the fast marching method. To reduce errors attributed to using local feature (intensity gradient) measurements, they used an average intensity gradient-based measure in the speed term. The method was applied to a parasternal short axis and an apical four-chamber view sequence but the results were only discussed qualitatively.

4. Classification of Ultrasound Segmentation Based On Methods Applied

Due to the relatively low quality of clinical ultrasound images, a good ultrasound image segmentation method needs to make use of all task-specific constraints or priors.

4.1 Speckle Noise or Features

Traditionally, speckles in an ultrasound image were treated as noise and algorithms were proposed to reduce them. More recent studies used speckles to measure tissue displacement and optimize image registration. Speckle gives ultrasound images their characteristic granular appearance. It inherently exists in coherent imaging, including ultrasound imaging.

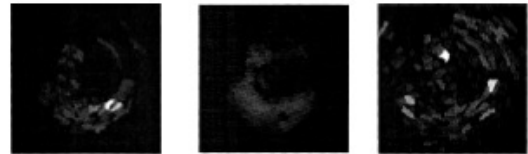
The received echo signals are obtained by a coherent summation of echo signals from many ultrasound scatterers. Speckle has a random and deterministic nature as it is formed from backscattered echoes of randomly or coherently distributed scatterers in the tissue. It has been shown that the statistical properties of the received signal, and thus of the echo envelope, depend on the density and the spatial distribution of the scatters [1]. Several distribution families have been proposed in the literature. For the special case of a large number of randomly located scatterers, the statistics of the envelope signal shows a Rayleigh distribution (see e.g. [1]). In this condition, the speckle is called fully developed. Deviations from such special scattering conditions have been previously modeled via The Rice distribution to account for a coherent component due to the presence of a regular structure of scatterers within the tissue.

The K-distribution to account for low effective scatter density (partially developed speckle). Unfortunately, the Rician family fails to account for reduced scatterer densities, and the χ^2 -distribution model does not take into account the presence of a coherent component. General models have been proposed in the literature namely the generalized K-distribution and the homodyned K-distribution and most recently the Rician Inverse of Gaussian distribution. The three models are general and can account for the different scattering conditions. However, the analytical complexity with these families is significant. Some effort has been put into efficiently estimating the parameters and alternative simple models have also been proposed such as the Nakagami family.

Figure 5 shows the results of the speckle statistics, where each pixel of AOI is assigned the value calculated from the ridge tree at which the pixel's outgoing stream ends.

There is also an extensive literature on speckle reduction which has been proposed as a pre-segmentation step; recent works include wavelets-based methods anisotropic diffusion methods.

(a) Speckle ridge Tree Size (b) Speckle average ridge gray-scale (c) Speckle weighted gray scale



4.2 Image Process

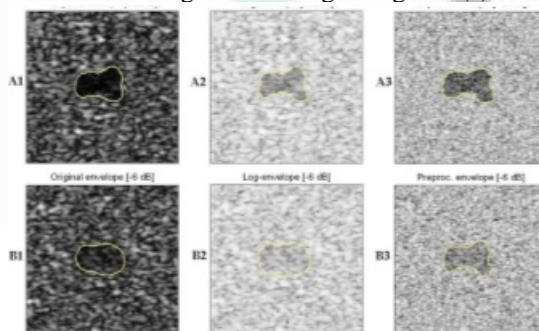
In this section we focus on non-textured based models including image differencing, histogram analysis, morphology, masking and active contours. Speckle data could be categorized into two groups: Boundary Speckles, which represent existing physical boundaries varying in size and distance, and Random Speckles, usually smaller in size representing no real object. We have further subdivided this definition within our research, to Elongated Speckles (with striated sheath structures) tending to represent tendon internals, and Dot Speckles tending to represent tissue (Figure 6(a)).

Klingler et al. [3] presented a semiautomatic technique applying mathematical morphology to segment the endocardium in echocardiograms. A morphological opening filter of radius size 20 was applied to a composite frame (the average of all frames), which removed intensity peaks in the image. The resultant image was then subtracted from the original, retaining edge information partially corrected for grayscale variation, followed by grayscale closing and binary dilation. They extracted a closed contour by iteratively thinning the result, identifying the contour as the inside edge of the endocardium, and proceeded with boundary enhancements. These techniques have been researched in many radiological procedures including elastography and angiography. For example, Benkeser et al. used elastography tools to measure tissue displacement under an

axial stress and extracted relevant features using binary thresholding and dilation / erosion operators. Figueiredo and Leitaó applied a Bayesian framework for estimating a ventricular contour to pre-processed angiographic images. Images of before and after an injection of a contrast agent were subtracted, removing any occluding osseous structures and leaving only vessels. Bouma et al. also implemented this classic process of calculating a background image and applying morphology and image subtraction for segmenting vessels from intravascular ultrasound images.

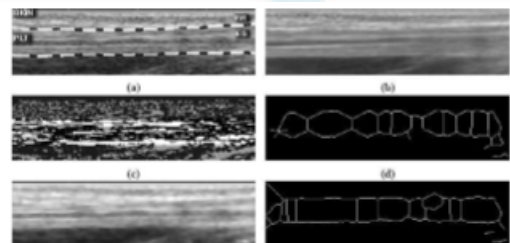
J.D. Revella, M. Mirmehdian and D. McNally, "Applied review of ultrasound image feature extraction methods" Initially, they performed image differencing after producing a composite frame from 20 of our sequential images (Figure 6(b)). Then the composite and single frames were subtracted, and using a grey level threshold obtained empirically, and produced a binary image. The output highlighted the tendon edges poorly, but emphasized existing internal sheath regions that could later be used for landmarking experiments (brighter central regions in Figure 6(c)). Next, they created a flat binary matrix defining the neighbourhood of a disk-shaped structured element with radius 4. They used a disk-shape as a result of our earlier definition of Dot Speckle characteristics (Klinger et al. used a hexagon structure sometimes leading to errors). Then performed morphological opening by eroding the composite frame with our disk structure to remove, by iterative reduction, hyperechoic Dot Speckle intensity regions, and applied a final binary dilation for restoration. To extract the final contour we iteratively thinned the image giving comparable results to, but failed to accurately extract tendon features for use in their application (Figure 6(d)). Additionally, we extended our analysis by applying anisotropic diffusion [81] with 10 iterations as shown in Figure 6(e) that proved effective for smoothing speckle regions while preserving and enhancing the contrast at sharp intensity gradients. Figure 6(f) shows much better edge features from applying iterative thinning to the thresholded diffusion output, with longitudinal lines displaying the approximate outside edges of the tendon.

(a) Hand labelled original ROI: Pulmarus Longus Tendon (PLT) dotted boundary and Elongated Speckle (ES) and Dot Speckle (DS) regions, (b) composite frame, (c) image subtraction (Frame 1 Motion), (d) Klingler et al's approach, (e) anisotropic diffusion, (f) final output, after thresholding and thinning of Figure 6(e).



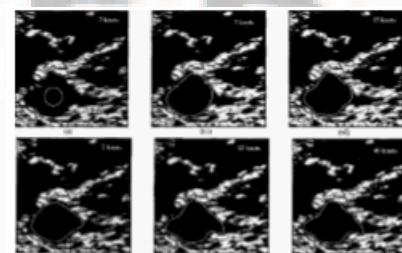
4.3 Active Contours

Present study demonstrates that the performance of segmentation algorithms can be substantially improved via applying the latter to preprocessed rather than original images. In particular, the proposed method segments ultrasound images in the logarithmic domain, after the images have been subjected to the processes of decorrelation and outlier shrinkage. It is shown that this preprocessing is capable of considerably improving the separability of segmentation classes, thereby increasing the accuracy of resulting segmentation. The method by means of which the segmentation is performed is based on the technique of active contours. The method uses the concept of combining multiple trajectory models in order to track a single target in a randomly distributed cluttered environment. In the previous original work by the authors, a PDAF technique was used to extract carotid artery contours from a sequence of ultrasound images in real-time. In the current work, we combine the PDAF technique with the IMM estimator in order to increase the accuracy of the extracted contours. This combination has been necessary, since in contrast to the carotid artery that has a well-defined circular shape, prostate boundary can have almost any arbitrary shape and come in different sizes. Because of the low computational cost of the algorithm, it has a great potential to be implemented for real-time applications. (A1-A3) Segmentation of the original, log-, and preprocessed envelopes at -12 dB contrast; (B1-B3).



4.4 B-Spline

A snake is a curve that evolves from an initial position towards the boundary of an object, minimizing some energy functional. Such functional consists of two terms: the internal energy and the external energy. The first term affects the smoothness of the curve, Segmentation of the original, log-, and preprocessed envelopes at -6 dB contrast.



Result of the proposed B-spline snake segmentation for different number of knots and parameters while the second attracts the snake towards image features. Splines can be effectively integrated in the snakes model, as they can characterize a continuous parametric curve by a vector of control points [89]. The benefit of using splines comes

from the implicit properties of the model, including the local support and the control of the continuity of the curve. The functional defining the energy of a B-spline having the equation $s(u) = (x(u), y(u))$ is:

$$E_{snake} = E_{intern}(s(u)) + E_{extern}(s(u))$$

5. Conclusions

Here we discussed the formation of Ultrasound Images and their advantages in the medical field. Because of increasing applications in the field of ultrasound images in diagnosis as well as therapeutic purposes we need to enhance the feature which we require for further processing. There are different techniques for doing this. One of these is segmentation which is a wide area of image processing. So in the other section we briefly discussed the segmentation methods.

After getting the idea about segmentation and ultrasound images we discussed different techniques and papers on the basis of particular clinical application as well as on the basis of methods used to segment out the ultrasound images.

References

- [1] J A Noble "Ultrasound Image Segmentation and Tissue Characterization," Part H: J. Engineering in Medicine, vol. 223, pp. 1-10, June 2009.
- [2] Mishra, P. K. Dutta, and M. K. Ghosh, "A GA based Approach for Boundary Detection of left Ventricle with Echocardiographic Image Sequences," Image Vis. Computational., vol. 21, pp. 967-976, 2003.
- [3] J.Klingler, J. Vaughan, T. Fraker et al. "Segmentation of Echocardiographic Images using Mathematical Morphology," IEEE Trans. on Biomedical Engineering 35, pp. 925-934, 1988.
- [4] Y. Zimmerand, R. Tepper and S. Akselrod. "A two-dimensional Extension of minimum Cross Entropy Thresholding for the Segmentation of Ultrasound Images," Ultrasound Medical. Biological, vol 22, pp.1183-1190, 1996 .
- [5] G. Coppini, R. Poli, and G. Valli. "Recovery of the 3-D shape of the left ventricle from Echocardiographic Images," IEEE T. Med. Imag., vol.14, pp.301-317, 1995.
- [6] T.N. Jones and D.N. Metaxas. "Segmentation using Deformable Models with Affinity-based localization," Lecture Notes in Computer Science, vol-1205, pp.53-52, 1997.
- [7] D. Kucera and R.W. Martin. "Segmentation of Sequences of Echocardiographic Images using a Simplified 3D Active Contour Model with region based External forces," Comput. Med. Im. Graph, vol-21, pp-1-21, 1997.
- [8] F. Lefebvre, G. Berger, and P. Laugier. "Automatic Detection of the Boundary of the Calcaneus from Ultrasound Parametric Images using an Active Contour Model," clinical assessment. IEEE T. Med. Imag, vol- 17, pp.45-52, 1998.
- [9] S.D. Pathak, P.D. Grimm, V. Chalana, and Y. Kim. "Pubic Arch Detection in Transrectal Ultrasound Guided Prostate Cancer Therapy," IEEE T. Med. Imag., vol-17 ,pp. 762-771, 1998.
- [10] S.D. Pathak, V.Chalana, and Y.M. Kim. "Interactive Automatic Fetal Head Measurements from Ultrasound Images using Multimedia Computer Technology," Ultrasound in Medicine and Biology, vol-23, pp .665-673, 1997